N-Glycans Modulate the Function of Human Corticosteroid-Binding Globulin*[S]

Zeynep Sumer-Bayraktar‡, Daniel Kolarich§¶, Matthew P. Campbell§, Sinan Ali‡, Nicolle H. Packer§, and Morten Thaysen-Andersen§‖

Human corticosteroid-binding globulin (CBG), a heavily glycosylated protein containing six *N*-linked glycosylation sites, transports cortisol and other corticosteroids in blood circulation. Here, we investigate the biological importance of the *N*-glycans of CBG derived from human serum by performing a structural and functional characterization of CBG *N*-glycosylation. Liquid chromatography-tandem MS-based glycoproteomics and glycomics combined with exoglycosidase treatment revealed 26 complex type *N*-glycoforms, all of which were terminated with α2,3-linked neuraminic acid (NeuAc) residues. The CBG *N*-glycans showed predominantly bi- and tri-antennary branching, but higher branching was also observed. *N*-glycans from all six *N*-glycosylation sites were identified with high site occupancies (70.5–99.5%) and glycoforms from all sites contained a relatively low degree of core-fucosylation (0–34.9%). CBG showed site-specific glycosylation and the site-to-site differences in core-fucosylation and branching could be *in silico* correlated with the accessibility to the individual glycosylation sites on the maturely folded protein. Deglycosylated and desialylated CBG analogs were generated to investigate the biological importance of CBG *N*-glycans. As a functional assay, MCF-7 cells were challenged with native and glycan-modified CBG and the amount of cAMP, which is produced as a quantitative response upon CBG binding to its cell surface receptor, was used to evaluate the CBG:receptor interaction. The removal of both CBG *N*-glycans and NeuAc residues increased the production of cAMP significantly. This confirms that *N*-glycans are involved in the CBG:receptor interaction and indicates that the modulation is performed by steric and/or electrostatic means through the terminal NeuAc residues. ***Molecular & Cellular Proteomics 10: 10.1074/mcp.M111.009100, 1–14, 2011.***

Human corticosteroid-binding globulin (CBG)[1], also referred to as transcortin in the literature, is the major plasma transport protein that binds cortisol and progesterone with high affinity in a single steroid binding site, providing a reservoir for the circulating steroids and regulating the amount of free hormones that are available for entry into target tissues (1, 2). The primary sequence and the recently solved three-dimensional structure of (modified) human CBG confirm that CBG structurally, but not functionally, is homologous to members of the serine protease inhibitor superfamily (3, 4). The release of bound cortisol at sites of inflammation is promoted by an elastase-induced cleavage of a reactive center loop of CBG resulting in a conformational change that favors the release of steroid from the binding pocket (5, 6). A number of reports have demonstrated that CBG binds to high-affinity receptors on the surface of various cell types (7–10). Although no receptor has been fully characterized to date, the CBG:receptor interaction is known to induce an accumulation of cAMP as a secondary messenger in different cells (8, 11, 12). The CBG:receptor interaction is also associated with the targeted delivery of steroids to specific cell types; however, the exact mechanisms behind this have not been elucidated.

CBG has six *N*-linked glycosylation sites and although a considerable effort has been put into increasing the understanding of the CBG glycosylation, the detailed structure and function relationship of the CBG *N*-glycans remains largely unknown. From monosaccharide composition analysis it has been established that CBG is conjugated with complex type *N*-glycans showing terminal sialylation and fucosylation on bi- and tri-antennary structures (13, 14). Also, *N*-glycans with higher branching have been suggested and it has been estimated that approximately five moles *N*-glycan occupy one mole CBG. However, a site-specific characterization of CBG *N*-glycans has not been performed and little is known on the monosaccharide compositions and relative abundances of the glycoforms from the six CBG glycosylation sites and the site-specific *N*-glycan occupancies.

Several studies have investigated the biological importance of *N*-glycans for the function of CBG. The motivation for this has in part been catalyzed by the finding of phylogenetically conserved CBG glycosylation sites (15) and the identification

From the Department of ‡Biological Sciences and §Chemistry and Biomolecular Sciences, Macquarie University, Sydney, NSW 2109, Australia

Received February 24, 2011, and in revised form, April 18, 2011
Published, MCP Papers in Press, May 10, 2011, DOI 10.1074/mcp.M111.009100

[1] The abbreviations used are: CBG, corticosteroid-binding globulin; BPC, base peak chromatogram; ETD, electron transfer dissociation; FA, formic acid; Gal, galactose; GlcNAc, *N*-acetylglucosamine, HILIC, hydrophilic interaction chromatography; LacNAc, *N*-acetyllactosamine, NeuAc, *N*-acetylneuraminic acid; XIC, extracted ion chromatogram; RT, room temperature; LC-MS/MS, liquid chromatography-tandem MS; ACN, acetonitrile; TFA, trifluoroacetic acid; ESI, electrospray ionization; CID, collision-induced dissociation.

of physiology-dependent glycosylation variants of CBG (16, 17). For example, it was reported that a pregnancy-associated glycosylation variant of human CBG has a higher degree of sialylation, branching, and occupancy than normal CBG (18–21). Importantly, some of the glycosylation variants have been shown to affect the function of CBG *e.g.* pregnancy-associated CBG has significantly lower affinity for one class of binding sites on placental syncytiotrophoblasts compared with normal CBG. Interestingly, this variant also shows substantially higher binding to other membrane preparations compared with normal CBG, indicating the presence of multiple CBG receptors with different binding preferences on some cell surfaces (22, 23). In another study, it was shown that CBG *N*-glycans are essential for the biosynthesis of CBG that has steroid-binding activity (24). Later it was specified that it is the Asn^{238} *N*-glycans (glycosylation site 4) that are required for the production of CBG with steroid binding properties (25–27). In addition, it was established that the *N*-glycans on this site are not needed for steroid binding after the protein has been folded to its mature conformation. Finally, terminal *N*-acetylneuraminic acid (NeuAc) residues of CBG *N*-glycans have been related to prolonged half-life in circulation (28) and it has been shown that *N*-glycosylation is important for stability and secretion of CBG (25, 26, 29). However, the majority of the above-mentioned studies have used recombinant human CBG (*e.g.* human CBG produced in CHO cells, insect cells, or in human cell lines) in various assays to document the function of the CBG *N*-glycans. This might have resulted in inaccurate conclusions because protein glycosylation is known to be highly species-, cell- and condition-dependent (30–32), emphasizing the need to use purified native human CBG for such studies.

The aim of this study was to investigate the biological importance of the *N*-glycans of naturally occurring human CBG isolated from pooled human serum by detailed glycomics, glycoproteomics, and functional characterization.

EXPERIMENTAL PROCEDURES

Origin of CBG—Affinity purified human CBG (Acc. No: P08185) isolated from a large pool of human serum from healthy adult donors was obtained from Affiland, Belgium. High purity of CBG was shown using SDS-PAGE and intact mass matrix-assisted laser desorption ionization (MALDI) MS (see Fig. 4). CBG was stored at a concentration of 1 μg/μl in 20 mM Tris- HCl, pH 7.4 at −20 °C until used.

Proteolytic Digestions—The cysteine residues of CBG were reduced by incubation for 45 min at 56 °C in 10 mM dithiothreitol (final concentration) and subsequently carbamidomethylated by incubation for 30 min in the dark at room temperature (RT) in 20 mM iodoacetamide (final concentration). The reaction was quenched by 20 mM dithiothreitol (final concentration). CBG was sequentially digested using 5% (w/w) sequence-grade trypsin (porcine, Promega, Madison, WI) (incubation condition: 50 mM NH_4HCO_3, pH 7.8, 10 h, 37 °C) and then 1% (w/w) endoproteinase Asp-N (*Pseudomonas fragi,* Roche) under the same incubation conditions. In a separate experiment, a proteolytic digest of reduced and alkylated CBG was performed using 2.5% (w/w) endoproteinase Asp-N alone under identical conditions. Aliquots of ~20 pmol digested CBG were stored at −20 °C until used. For direct LC-MS/MS analysis, an aliquot was dried and taken up in 20 μl aqueous 0.1% (v/v) formic acid (FA).

Glycopeptide Enrichment—Before liquid chromatography-tandem MS (LC-MS/MS) analysis, a fraction of the trypsin/Asp-N peptide mixture (20 pmol) was enriched for glycopeptides. This sample was dried and taken up in 10 μl 80% (v/v) acetonitrile (ACN) in aqueous 0.1% trifluoroacetic acid (TFA). The glycopeptide enrichment was carried out using hydrophilic interaction chromatography (HILIC) in micro-column format. The stationary phase consisted of ZIC-HILIC resin (10 μm particle size, 200 Å pore size, kindly provided by Sequant/Merck, UmeÅ, Sweden). The microcolumns were prepared as previously described (33, 34). In brief, the HILIC resin was packed in a GeLoader tip (Eppendorf, Hamburg, Germany) to form a microcolumn (height: 10 mm, column volume: ~0.3 μl) and equilibrated in 20 μl mobile phase consisting of 80% (v/v) ACN, aqueous 0.1% TFA. After sample loading, the column was washed twice with 10 μl mobile phase before the retained glycopeptides were eluted with 10 μl 2% (v/v) aqueous FA. This fraction was dried and taken up in 20 μl 0.1% (v/v) FA and used for multiple LC-MS/MS injections.

Glycomics—CBG was immobilized in four discrete spots (3 μg/spot) on a primed and blocked 0.45 μm Immobilon- PSQ polyvinylidene difluoride membrane (Millipore, Billerica, MA) and processed as described previously (35). In brief, these spots were stained with Direct Blue (Sigma-Aldrich), excised and washed in separate wells in a flat bottom polypropylene 96-well plate (Corning, Corning, NY). The *N*-glycans were released from the membranes of all spots using 2.5 U PNGase F (*Flavobacterium meningosepticum,* Roche) in 10 μl water/well and incubation for 16 h at 37 °C. Before PNGase F release, three of the four spots were treated 10 h at 37 °C with the following exoglycosidases in 10 μl water: 1) 10 mU α-2,3-specific neuraminidase (*Streptococcus pneumoniae,* Sigma), 2) 20 mU broad specificity neuraminidase (*Clostridium perfringens,* Sigma), and 3) combination of 20 mU broad specificity neuraminidase (*Clostridium perfringens,* Sigma) and 250 mU β-1,4-specific galactosidase (*Aspergillus oryzae,* ProGlycAn, Austria). To remove the glycosylamines from the reducing end of the released *N*-glycans and allow for quantitative reduction, 10 μl 100 mM ammonium acetate, pH 5 was added and the mixtures incubated for 1 h at RT. Subsequently, the samples were dried and reduced to alditols by redissolving the *N*-glycans in 20 μl 1 M $NaBH_4$ in 50 mM KOH and incubation for 3 h at 50 °C. After neutralization with 2 μl glacial acetic acid, the *N*-glycans were desalted on cation exchange columns. The cation exchange resin (25 μl column volume, AG 50W X8, Bio-Rad, Hercules, CA) was packed onto a PerfectPure C-18 tip (Eppendorf, Hamburg, Germany), washed with 3 × 50 μl 1 M HCl, 3 × 50 μl methanol and then with 3 × 50 μl water before the sample was added. The flow-through from the sample load and two washing steps with 50 μl water were pooled. The samples were dried and then washed 5 times with 100 μl methanol to remove residual borate. Finally, each sample was redissolved in 10 μl water and analyzed with LC-MS/MS.

Mass Spectrometry—CBG peptide mixtures were analyzed by electrospray ionization (ESI)-MS in positive polarity mode on an HCT 3-D ion trap (Bruker Daltonics, Newark, DE) coupled to an Ultimate 3000 LC (Dionex). The samples were loaded directly onto a ProteCol C18 column (300 μm ID, 10 cm, particle size: 3 μm, pore size: 300 Å, SGE, Australia) equipped with an 0.5 μm peek filter (Upchurch, Oak Harbor, WA). The column was equilibrated in 100% solvent A (aqueous 0.1% (v/v) FA), the sample loaded and a gradient up to 50% (0.8%/min slope) solvent B (0.1% (v/v) FA in ACN) was applied before washing the column in 80% B for 10 min and re-equilibration in starting conditions. A constant flow-rate of 5 μl/min was used. The peptide mixtures were analyzed with and without glycopeptide enrichment and two injections (1–5 pmol/injection) were performed for each of the samples using different setups: 1) LC-MS/MS analysis,

where a MS full scan (*m/z* 400–2200, scan speed: 8100 *m/z*/sec) was followed by a data dependent fragmentation of the two most abundant signals using alternating CID and electron transfer dissociation (ETD) (ICC target 200,000 (max acc. time: 200 ms), ICC reactant target ETD: 600,000, reactant acc. time: 7–20 ms (max 200 ms), reaction time: 150 ms) and 2) LC-MS analysis, where only MS full scans (*m/z* 400–2200) were performed (ICC target 200,000, max acc. time: 200 ms). The LC-MS/MS analysis was used for site-specific characterization of CBG glycoforms and the LC-MS analysis was used to determine the site-specific (relative) quantities and occupancies of the glycoforms.

Released *N*-glycans (alditols) were separated on Hypercarb porous graphitized carbon column (5 μm particle size, 320 μm (ID) $\times$ 10 cm, Thermo Scientific) on an Agilent 1100 capillary LC (Agilent Technologies, Santa Clara, CA) and analyzed using an Agilent MSD three-dimensional ion-trap XCT Plus mass spectrometer coupled directly to the LC. Separation was carried out at a constant flow rate of 2 μl/min using a linear gradient with 2–16% (v/v) ACN/10 mM NH_4HCO_3 for 45 min, followed by a gradient from 16–45% over 20 min before washing the column with 45% (v/v) ACN/10 mM NH_4HCO_3 for 6 min and re-equilibrating in 10 mM NH_4HCO_3. ESI-MS was performed in negative ion mode with two scan events: MS full scan with mass range *m/z* 100–2000 and data dependent MS/MS scan after collision-induced dissociation (CID) of the top three most intense precursor ions.

For intact protein mass measurements of native and modified CBG, desalting was performed on custom-made Poros R1 (Applied Biosystems) microcolumns as previously reported (36). The glycoproteins were coeluted with matrix onto the target using 0.8 μl sinapic acid (20 g/l in 70% (v/v) ACN, 5% aqueous FA). The dried spots were mass analyzed using a MicroFlex (Bruker Daltonics) in linear mode with positive polarity ionization. All the mass spectrometers were externally calibrated using tune-mix (Agilent) for the ESI-MS instruments and intact bovine serum albumin (Sigma) for the MALDI-time-of-flight MS instrument.

Characterization, Quantitation, and Occupancy of CBG N-glycoforms—Initially, the monosaccharide compositions of the CBG *N*-glycans were manually determined from the glycomics and glycoproteomics LC-MS/MS data. Based on this, a catalog of 36 related (observed and hypothetical) monosaccharide compositions was created (See supplemental Fig. S1) and used to search the glycoproteomics data for glycopeptide glycoforms in GlycospectrumScan (www.glycospectrumscan.org) (settings: average glycopeptide mass, precursor mass accuracy: $\pm$0.5 Da, search for all charge states, identification threshold manually set to exclude noise peaks). For each of the six CBG glycosylation sites, MS peak lists were generated using Compass DataAnalysis 4.0 (Bruker Daltonik, Peak finder settings: signal-to-noise (S/N) threshold: 1, relative intensity threshold 0.1% of base peak, absolute intensity threshold: 100) by averaging the MS full scans for the respective glycopeptide eluting region (manually identified from LC-MS/MS data, see Fig. 2 for an example) and smoothing the resulting spectrum 0.2 Da (Gauss algoritm, 1 cycle). The elution windows were: Site 1: 32.5–34.5 min, Site 2: 57.0–61.0 min, Site 3: 50.0–53.0 min (Asp-N digest only), Site 4: 70.0–77.0 min, Site 5: 41.0–43.0 min, and Site 6: 53.0–55.5 min. The glycopeptide glycoform identifications were manually filtered based on relatedness, observed charge states, and mass accuracy. The identities of the glycopeptides were manually validated using CID and ETD fragmentation data. Based on this, both the *N*-glycan and peptide moieties as well as the glycosylation site could be confirmed. The site-specific relative quantitation of the glycopeptides was based on the peak intensity of the smoothed isotopic envelope of the glycopeptide precursor ions by assuming equal ionization efficiencies among the differently glycosylated peptides, which has shown to be a good approximation for populations consisting of sialoglycopeptides (37, 38). Hence, glycopeptide-based site-specific glycoprofiling has been shown to be highly accurate and excellent in terms of analytical reproducibility for both MALDI and ESI-MS based setups (38, 39). In the present study we used CBG purified from pooled human serum to determine the "average" human serum CBG glycoprofile rather than investigating the individual variability.

The detailed CBG *N*-glycan structures were manually determined from the glycomics experiments by their corresponding fragmentation in MS/MS, their relative LC retention time and by treatment with exoglycosidases (see above).

The *N*-glycan occupancies on the individual glycosylation sites were determined from the glycoproteomics LC-MS/MS analysis of the nonenriched samples to allow peptides with and without the attached *N*-glycans to be observed simultaneously. The occupancies were manually determined from the ratio of the extracted ion chromatogram (XIC) areas for all the charge states of the nonglycosylated and glycosylated (*i.e.* BS2) glycopeptides and relating this ratio to the determined site-specific glycoprofile. This assumes similar ionization efficiencies of the non-glycosylated and glycosylated glycopeptides, and a potential ionization bias toward the non-glycosylated glycopeptide was shown to be negligible by observing close-to-complete occupancies of some CBG glycosylation sites.

CBG Glycosylation Analogs—CBG glycosylation analogs were enzymatically generated under mild conditions (neutral pH, relative low temperature and salt concentration) to ensure retention of the activity of the glycoprotein. To allow direct comparison, all analogs were incubated under the same conditions *i.e.* total incubation time (39 h), temperature (37 °C), and buffer (20 mM Tris-HCl, pH 7.4), but with different enzymes and enzyme treatment periods. First, a partially deglycosylated analog (CBG_{Degly}), was generated by incubating CBG (1 μg/μl in 20 mM Tris-HCl, pH 7.4) at 37 °C for 22 h without enzyme and then at 37 °C for 17 h with 0.4 U PNGase F (*Flavobacterium meningosepticum,* Roche) per μg CBG. In addition, two partly desialylated CBG analogs were generated ($CBG_{Desia\ 1}$ and $CBG_{Desia\ 2}$). $CBG_{Desia\ 1}$ was generated by incubating CBG (1 μg/μl in 20 mM Tris-HCl, pH 7.4) at 37 °C for 35 h without enzyme and then at 37 °C for 4 h with 8 mU neuraminidase (*Clostridium perfringens,* Sigma) per μg CBG. $CBG_{Desia\ 2}$ was generated by incubating CBG (1 μg/μl in 20 mM Tris-HCl, pH 7.4) at 37 °C for 22 h without enzyme, then at 37 °C for 4 h with 8 mU neuraminidase per μg CBG and finally at 37 °C for 13 h with another 12 mU neuraminidase per μg CBG. Furthermore, a fully deglycosylated CBG analog ($CBG_{Desia/Degly}$) was prepared by first incubating CBG (1 μg/μl in 20 mM Tris-HCl, pH 7.4) at 37 °C for 4 h with 8 mU neuraminidase per μg CBG, then at 37 °C for 13 h with another 12 mU neuraminidase per μg CBG and finally at 37 °C for 22 h with 0.8 U PNGase F per μg CBG. As controls, CBG (1 μg/μl in 20 mM Tris-HCl, pH 7.4) was incubated at 37 °C for 39 h without any enzyme (CBG_{Incub}) and without any incubation at all (CBG_{Nat}). Following incubation the glycosylation analogs were used immediately in the functional assay and a fraction of each sample was monitored using SDS-PAGE and intact mass MALDI MS analysis. For the SDS-PAGE, ~2 μg of the individual CBG glycosylation analogs were mixed with denaturing and reducing sample buffer (1:3 ratio), boiled for 5 min, analyzed on a 12% separation gel with a 4% stacking gel and stained with Coomassie Brilliant Blue R250. Intact mass MALDI MS was performed as described above.

Functional Assay—Human breast cancer MCF-7 cells were used in the functional assay as these have been shown to bind CBG and generate a dose- (CBG) and time-dependent cAMP response (12). The MCF-7 cell line was grown using T175 EasYFlasks™ (Nunc) at 37 °C, 5% CO_2 and 95% humidity in Roswell Park Memorial Institute (RPMI) 1640 Medium (Sigma) supplemented with 10% (v/v) fetal calf serum, 0.1% (w/v) Penicillin G, 0.2% (w/v) Kanamycin, 1% (w/v) Amphotericin B Solution (all antibiotics were from Sigma). For the

functional assay, cells were transferred to 96-well tissue culture plate (Costar) and cultured with media containing supplements until they formed a monolayer and reached 90% confluence. Twenty-four hours before the challenges, media was changed to serum-free media to avoid the interference of serum proteins.

MCF-7 cells (4.5×10^5 cells/well) were incubated for 1 h at RT with 100 pmol native CBG/well, modified CBG/well or 20 mM Tris-HCl, pH 7.4 in the presence of 100 pmol cortisol (Siemens Diagnostic Solutions) in each well.

Challenge with all the analogs was performed in triplicates. Following challenge, intracellular cAMP was extracted by the lysis reagent provided in the Amersham Biosciences cAMP Biotrak™ Enzymeimmunoassay (EIA) System kit (GE Healthcare). The lysate was then transferred to the cAMP Biotrak™ assay plate and the cAMP concentration was measured in duplicate by competitive based enzyme immunoassay, according to instructions from the manufacturer and with the solutions provided in the kit. In brief, cAMP standards were prepared ranging from 12.5–3200 fmol. Then, 100 μl of each standard and lysate were distributed into the assay plate wells with an equal amount of diluted antiserum and the plate incubated for 2 h at 4 °C. This was followed by the addition of 50 μl cAMP-peroxidase conjugate into the wells and a further incubation for 60 min at 4 °C. Subsequently, the assay plate was aspirated and washed four times with wash buffer and immediately 150 μl TMB added for color development. The plate was covered and shaken on a mixer for 1 h at RT, and the reaction was quenched by adding 100 μl 1 M sulfuric acid. The optical density was determined at 450 nm (Multiskan EX, Thermo Scientific) and the cAMP amount determined by comparison to the cAMP standards.

Structural Modeling—The available crystal structure of modified human CBG complexed with cortisol (PDB: 2VDY) was viewed with RasMol Ver 2.7.5 (RasWin Molecular Graphics). To obtain the crystal structure recombinant human CBG was produced in a SUMO expression system with a truncation of the N terminus (Met^1- Met^{10}) of the mature protein and with a replacement of the reactive loop (4). The present glycosylation sites (*i.e.* site 2–5) were mapped on the structure and their accessibilities calculated using NACCESS (40). A probe with a 5 Å radius was rolled around the atomic surface of the protein to calculate atomic solvent accessible areas (41). NACCESS uses Van der Waals' radii (42). The relative accessibilities were determined from the solvent accessibilities to the formerly glycosylated asparagine residues only and the values normalized to the most accessible site (glycosylation site 2).

RESULTS

Structural Characterization of CBG N-Glycans—*N*-glycans of human CBG purified from pooled human serum were structurally characterized using both glycoproteomics and glycomics to obtain complementary *N*-glycan information. For the glycoproteomics approach, the peptide mixtures originating from both a sequential trypsin and endoproteinase Asp-N digest of CBG and a digest using Asp-N alone were analyzed using reversed-phase LC-ESI-MS/MS with and without prior glycopeptide enrichment using off-line hydrophilic interaction chromatography (HILIC) (See workflow, Fig. 1).

As expected, a relatively complex base peak chromatogram (BPC) was observed when the CBG peptide mixture was analyzed without enrichment, Fig. 2*A* (*top* chromatograms). However, glycopeptide-containing spectra could still be identified using XIC for the diagnostic *N*-glycan fragment ions at *m/z* 366.1 and *m/z* 657.2 (BY- and B-ions). Using this approach, glycopeptides originating from five of the six predicted CBG glycosylation sites could be identified. The remaining glycosylation site (site 3) was located in a dipeptide (Asn^{154}-Lys^{155}) that was poorly retained by reversed phase LC, thus explaining its absence in the analysis. Glycopeptides from this site were observed early in the gradient upon HILIC enrichment presumably because of substantial desalting of the sample and removal of interfering nonglycosylated peptides. However, the small glycopeptide was not suited for characterization, quantitation, or occupancy of *N*-glycans from this site and a separate digest using Asp-N alone was used for this purpose (Asn^{140}-Lys^{161}). The HILIC enrichment of *N*-glycopeptides proved to be extremely efficient as previously observed (33, 34), enabling a close-to-complete isolation of the glycopeptides Fig. 2*A* (*bottom* chromatograms). Importantly, the glycopeptides were isolated in a non-biased manner judging from the preserved ratio between glycopeptide signals from the individual sites in the two XIC chromatograms of before and after enrichment.

Site-specific Characterization of CBG Glycoforms—The well-separated glycopeptides originating from the six glycosylation sites were identified by summing the MS full scans of the eluting areas from the LC-MS/MS analysis of the HILIC enriched peptide mixture. Broad elution windows were allowed to include the complete set of peptide glycoforms. As an example, Fig. 2*B* shows the summed MS full scans for the LC elution time 57–61 min where glycopeptides originating from glycosylation site 2 elute. These glycopeptides were heterogeneously *N*-glycosylated and carried two to five positive charges, complicating the assignment further. The monosaccharide compositions of the glycoforms showed the presence of a wide range of complex type *N*-glycans and indicated structures with various branching *i.e.* bi- (B), tri- (T), tetra- (Te), and penta- or tetra + one *N*-acetyllactosamine (LacNAc) (P) antennary structures. In addition, all *N*-glycans were sialylated (S) carrying between one (S1) and six (S6) *N*-acetylneuraminic acid (NeuAc) residues. Finally, a proportion of the glycoforms appeared to be fucosylated (f).

The site-specific monosaccharide composition and topology information of the glycoforms were determined by manual assignment of the LC-MS/MS data. The characterization was based on the molecular mass and fragmentation of the *N*-glycopeptides. Both CID and ETD were used to give complementary information on the glycopeptides (43). As expected, CID generated predominantly fragmentation of the glycosidic bonds of the glycopeptides generating B- and Y-ions and some diagnostic oxonium ions providing information on the attached *N*-glycan (Fig. 2*C*). In contrast, c- and z- ions of the (glyco)peptide were observed upon ETD fragmentation yielding information about the peptide identity as well as glycosylation site.

Glycoprofiling of CBG Glycosylation Sites—From the site-specific analysis, the identities and relative abundances of the glycoforms attached to the six CBG glycosylation sites were

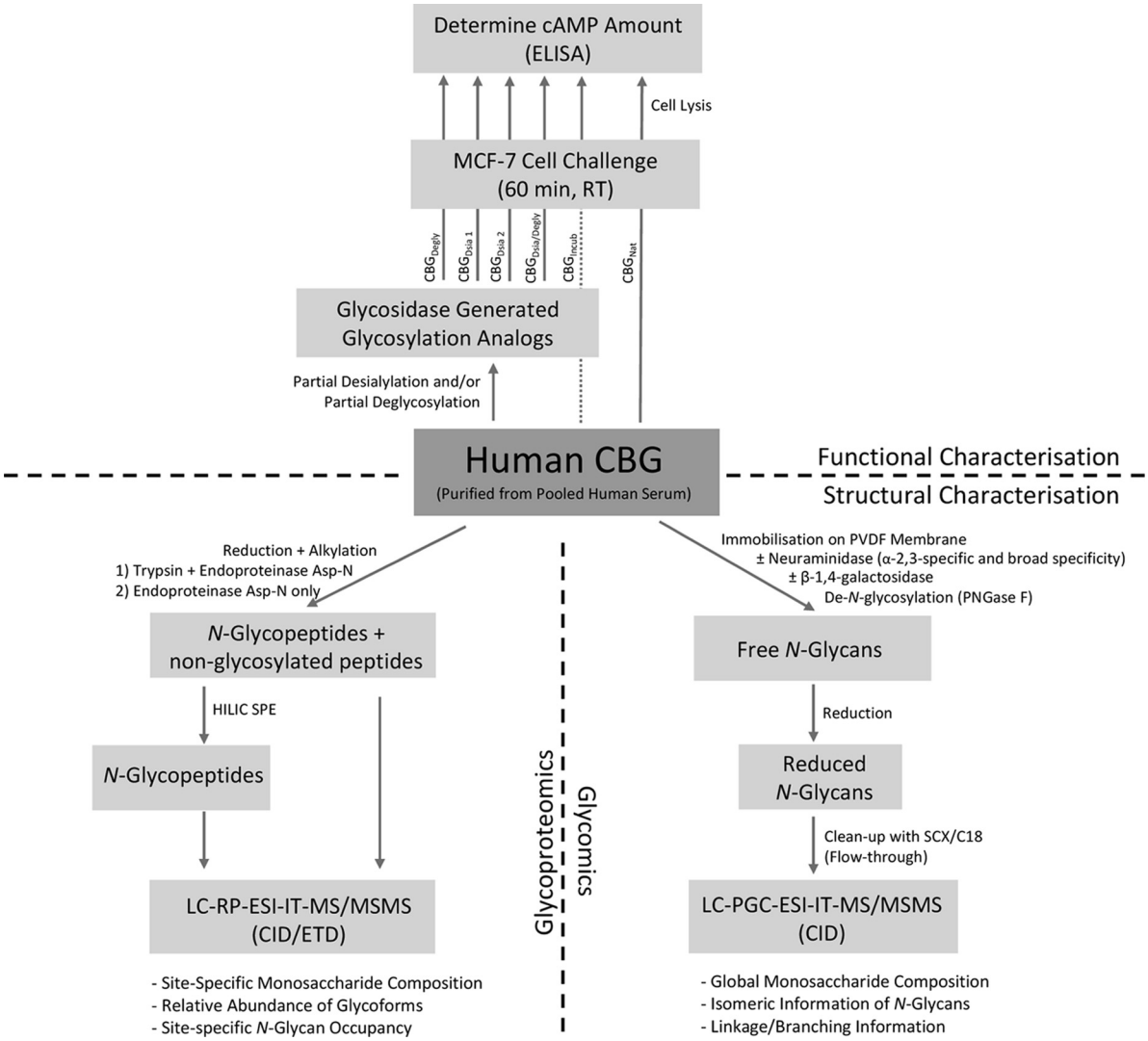

FIG. 1. **Workflow illustrating the experimental setup.** The *N*-glycans of human CBG were structurally characterized (*bottom half*) using glycoproteomics (*left*) and glycomics (*right*). Functionally, the CBG *N*-glycan involvement in the CBG:receptor interaction was investigated (*upper half*) by challenging MCF7 cells with native/heat exposed CBG (CBG_{Nat} and CBG_{Incub}) and glycosylation analogs (CBG_{Degly}, $CBG_{Desia\ 1}$, $CBG_{Desia\ 2}$, $CBG_{Desia/Degly}$) and monitoring the cAMP response, which has been shown to be an accurate measure to evaluate the CBG:receptor interaction.

determined, Table I. The glycan structures from the individual glycosylation sites were similar, but the glycoprofile varied considerably. Glycosylation site 2, 3, and 6 contained the most heterogeneity with the most processed set of complex glycoforms and glycosylation site 4 and 5 contained the least.

The relative quantitation of the glycoforms was determined from their mass spectral signal intensities of the complete set of observed charge states. This task was performed using our recently introduced bioinformatic tool, GlycoSpectrumScan (44). This relative quantitation method is based on the assumption of equal ionization efficiencies among the differently glycosylated peptides, which has shown to be a good approximation for populations consisting of sialoglycopeptides (37, 38). The nonfucosylated bi- and tri-antennary fully sialylated *N*-glycans (*i.e.* BS2 and TS3) were abundantly attached to all sites *i.e.* BS2: 11.6–79.2% and TS3: 10.0–37.8%. All 26 glycoforms were sialylated, but the degree of sialylation varied from 2.10 mol NeuAc/mol *N*-glycan (site 4) to 2.89 mol NeuAc/mol *N*-glycan (site 6), Table II. Taking the site-specific occupancies into consideration (see below), the global sialylation level of CBG was found to 13.3 mol NeuAc/mol CBG, which agrees well with other studies estimating 11.2–13.6 mol NeuAc/mol CBG (13, 20, 21). The degree of fucosylation varied from 0–34.9% between the sites, Table II. From this it is estimated that 0.76 mol fucose is attached to one mol CBG, which is in reasonable agreement with previous studies reporting 1.2–1.4 mol fucose/mol CBG (13, 20, 21).

CBG N-Glycan Occupancy—The *N*-glycan occupancies on the individual glycosylation sites were determined from the

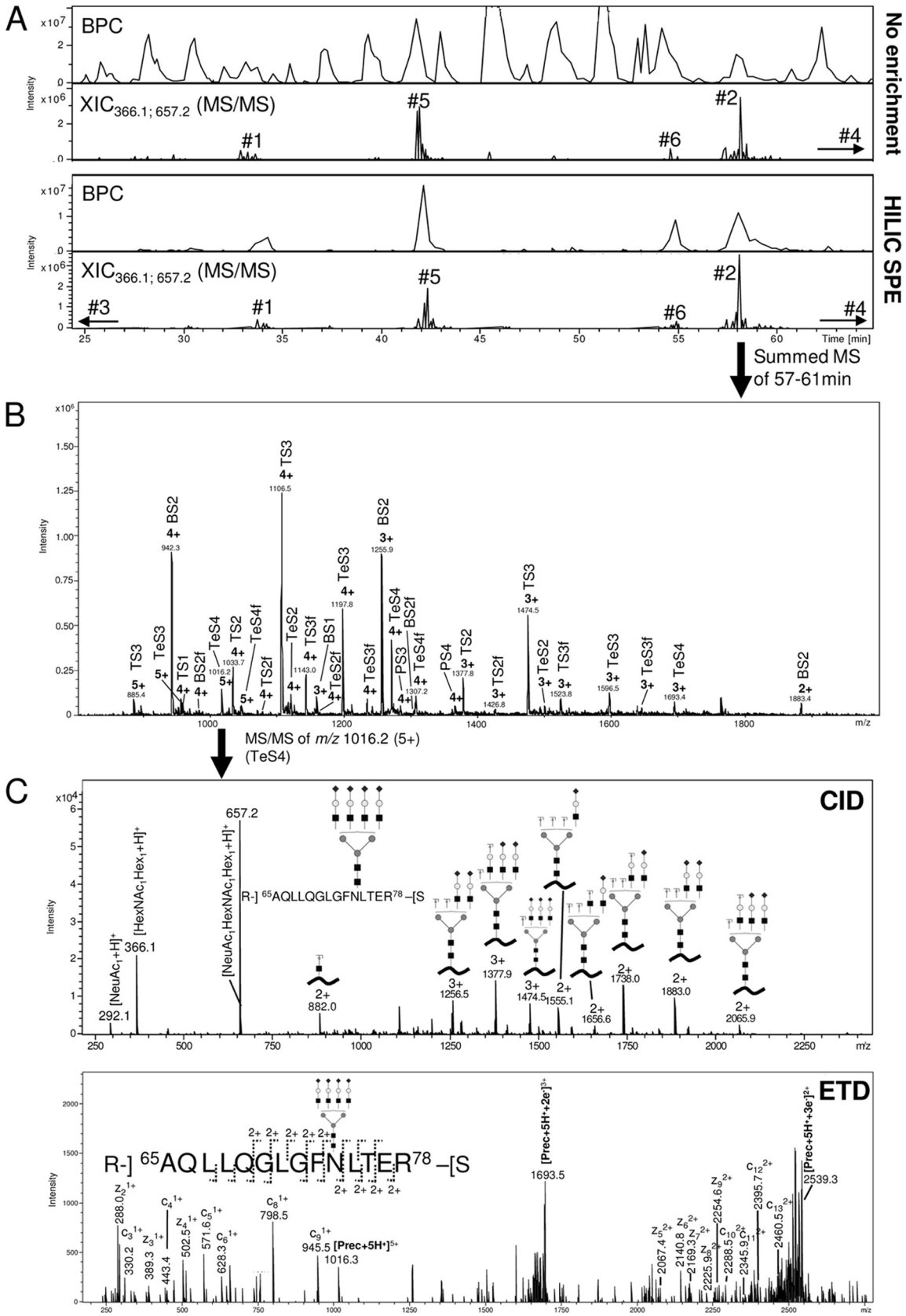
A
BPC
XIC366.1; 657.2 (MS/MS)
No enrichment
HILIC SPE
#1
#2
#3
#4
#5
#6
Time [min]
Summed MS of 57-61min
B
MS/MS of m/z 1016.2 (5+) (TeS4)
C
CID
ETD
R-] 65AQLLQGLGFNLTER78 –[S
[Prec+5H+]5+
[Prec+5H++2e-]3+
[Prec+5H+3e-]2+

TABLE I

Composition, underivatised residual glycan mass and relative abundance (in per cent) of the observed N-glycoforms based on site-specific profiling of glycopeptides. B: bi-antennary, T: tri-antennary, Te: tetra- antennary, P: penta-/tetra-antennary + one LacNAc extension, S: NeuAc, Gal: galactose, f: fucose, Hex: hexose, HexNAc: N-acetylhexoseamine, NeuAc: N-acetylneuraminic acid, Fuc: Fucose

Name	Composition				Glycan Mass (Residue)/Da	Glycopeptide profiling (Site)					
	Hex	HexNAc	NeuAc	Fuc		1	2	3	4	5	6
BS1-Gal	4	4	1	0	1751.62	2.6					1.0
BS1f-Gal	4	4	1	1	1897.68						0.7
BS1	5	4	1	0	1913.68		1.4	4.8		3.1	1.3
BS1f	5	4	1	1	2059.79			1.1			
BS2	5	4	2	0	2204.77	40.8	18.5	63.2	79.2	66.9	11.6
BS2f	5	4	2	1	2350.83	4.9	1.4	7.3		1.5	3.6
TS1	6	5	1	0	2278.81		2.0	0.3			
TS2	6	5	2	0	2569.90	4.0	5.9	1.6	10.8	2.1	3.5
TS2f	6	5	2	1	2715.96	1.3	1.2	0.4			2.3
TS3	6	5	3	0	2861.00	32.7	21.7	14.7	10.0	21.1	37.8
TS3f	6	5	3	1	3007.06	11.0	3.8	4.1		3.3	23.6
TS4	6	5	4	0	3152.10	0.8				2.1	4.0
TeS2	7	6	2	0	2935.04		4.2				
TeS2f	7	6	2	1	3081.09		0.7	0.4			
TeS3	7	6	3	0	3226.13	1.0	11.6	0.5			0.8
TeS3f	7	6	3	1	3372.19		2.7				0.7
TeS4	7	6	4	0	3517.23	0.9	17.8	0.9			2.9
TeS4f	7	6	4	1	3663.29		3.8				2.1
TeS5	7	6	5	0	3808.32		0.6				1.5
TeS5f	7	6	5	1	3954.38			0.4			0.6
PS3	8	7	3	0	3591.26		1.1				
PS4	8	7	4	0	3882.36		1.5				
PS4f	8	7	4	1	4028.42						0.6
PS5	8	7	5	0	4173.46						0.6
PS5f	8	7	5	1	4319.51						0.8
PS6f	8	7	6	1	4610.61			0.4			

LC-MS/MS analysis of the nonenriched sample to allow peptides with and without the attached *N*-glycans to be observed simultaneously. High *N*-glycan occupancies were found for all glycosylation sites ranging from 70.5% (Site 4) to 99.5% (Site 2), Table II. The occupancies were determined from the ratio of the XIC areas for all the charge states of the nonglycosylated and glycosylated (*i.e.* BS2) glycopeptides. Because of the analysis in positive polarity mode, this has the potential of introducing a bias toward the nonglycosylated glycopeptides (underrepresentation of the sialoglycopeptides) with the result of underestimating the *N*-glycan occupancies. However, the high occupancy determined for glycosylation site 2 (99.5%) illustrated that the bias is negligible, if present at all. In addition, summing the individual site occupancies, the total occupancy of 5.4 mol *N*-glycan/mol CBG agreed well with previous studies estimating 5.0–5.1 mol *N*-glycan/mol CBG (13–15).

Glycomics—Global profiling of the released CBG *N*-glycans was used to obtain further structural details. This was performed in a site-unspecific manner by enzymatically releasing the CBG *N*-glycans using PNGase F and analyzing their reduced derivatives (alditols) by ESI-LC-MS/MS on a porous graphitized carbon (PGC) column (See Flow Scheme, Fig. 1). The advantage of PGC-LC-MS/MS is that structural glycan isomers (isobaric and nonisobaric glycoforms) can be separated and that the relative retention time and fragmentation of *N*-glycans in negative ionization mode, which yields diagnostic ions, can aid the characterization of the specific *N*-glycan structures (45).

Single peak formation in XICs from the LC-MS/MS data (examples shown in supplemental Fig. S2) indicated the absence of isobaric glycoforms (*e.g.* α2,3- or α2,6-linked NeuAc isomers and core/Lewis- type fucose isomers) from the monosaccharide compositions shown in Table I. To determine the NeuAc-Gal linkage, CBG *N*-glycans were incubated with α2,3-specific neuraminidase prior to PNGase F release and analysis by LC-MS/MS. This generated a close-to-complete

FIG. 2. **Glycopeptide profiling using LC-MS/MS based glycoproteomics.** *A,* Base peak chromatograms (BPCs) and extracted ion chromatograms (XICs) (*m/z* 366.1 and *m/z* 657.2, fragment ions) for LC-MS/MS of non-enriched (top) and HILIC solid phase extraction (SPE) enriched (bottom) peptide mixture generated from a sequential trypsin/Asp-N digest of CBG. Glycopeptide eluting regions and their glycosylation site origins have been marked. A non-biased and close-to-complete isolation of glycopeptides was observed using off-line HILIC enrichment. *B,* Summed MS full scans of *N*-glycopeptides originating from glycosylation site 2. A relatively large elution window (*i.e.* 57–61 min) was allowed to ensure that the complete set of glycoforms was included. See 'Experimental procedures' for list of all elution windows. A heterogeneous set of glycoforms was observed (see Table I and Fig. 3 for nomenclature/structures). *C,* Examples of CID (upper) and ETD (lower) fragmentation of an *N*-glycopeptide originating from glycosylation site 2 (*i.e.* Ala^{65}-Arg^{78} conjugated with a tetra-antennary, fully sialylated complex *N*-glycan, *m/z* 1016.2, 5+).

MCP MOLECULAR & CELLULAR PROTEOMICS ASBMB

TABLE II

Glycosylation sites, (glyco)peptide sequences, non-glycosylated glycopeptide masses (Da), N-glycan occupancies, degrees of fucosylation, degrees of sialylation and distribution of branching as well as the relative accessibility to the individual glycosylation sites. These results are based on glycopeptide profiling

Glycosylation site (residue)	Glycopeptide (trypsin + Asp-N generated)	Non-glycosylated glycopeptide mass	N-Glycan occupancy	Degree of fucosylation	Degree of sialylation (mol NeuAc/mol *N*-Glycan)	Branching distribution (B:T:Te:P)[b]	Relative accessibility to site[c]
1 (Asn^{9})	Met^{1}-Arg^{15}	1755.76 Da	96.7%	17.2%	100% (2.45)	48:50:2:0	N/A
2 (Asn^{74})	Ala^{65}-Arg^{78}	1558.85 Da	99.5%	13.7%	100% (2.86)	21:35:41:3	1.00
3 (Asn^{154})	Asn^{154}-Lys^{155}	260.15 Da	89.0%[a]	14.1%[a]	100% (2.18)[a]	76:21:2:0[a]	0.80
4 (Asn^{238})	Asp^{223}-Pro^{246}	2740.32 Da	70.5%	0.0%	100% (2.10)	79:21:0:0	0.28
5 (Asn^{308})	Asp^{301}-Arg^{311}	1311.62 Da	96.3%	4.7%	100% (2.26)	71:29:0:0	0.23
6 (Asn^{347})	Asp^{337}-Arg^{356}	2056.15 Da	84.7%	34.9%	100% (2.89)	18:71:9:2	N/A
Global (CBG)			5.4 mol glycan/mol CBG	0.76 mol Fuc/mol CBG	13.3 mol NeuAc/mol CBG	51:38:10:1	

[a] The quantitation and occupancy of *N*-glycans from this glycosylation site were determined from a separate digest exclusively with endoproteinase Asp-N generating the (glyco)peptide Asp^{140}-Val^{161} (2506.33 Da).

[b] It was not possible to determine whether *N*-glycans with five LacNAc units attached to the core were a mix of penta-antennary and tetra-antennary structures with one LacNAc extension.

[c] See 'Experimental Procedures' and supplementary Fig. S4 for information on the relative accessibility to the individual glycosylation sites.

desialylation of the *N*-glycans suggesting that α2,3-linked NeuAc residues are abundantly attached to the penultimate Gal residues in the structures (supplemental Fig. S 2). A few over-sialylated glycoforms with more NeuAc residues than number of antennas were observed at very low abundance *e.g.* TS4, TeS5 and PS6. These additional NeuAc residues may be linked differently to the *N*-glycan, potentially as a α2,6-linkage to the *N*-acetylglucosamine (GlcNAc) of the antenna as observed for bovine fetuin (46). Because these species appeared with very low abundance it was not possible to clarify this further.

For the fucosylated glycoforms, fragment mass spectra were used to establish the location of the fucose residue, which in humans can be located either on the *N*-glycan core or on the antenna as Lewis-type antigens. The diagnostic fragment ion pair at *m/z* 350/368 (Z_1/Y_1) is indicative of the fucosylated, reduced *N*-acetylglucosaminitol, and was present in the fragment mass spectra of the fucosylated *N*-glycans (data not shown). This proved that the fucose residues are attached to the innermost GlcNAc as a core-fucosylation. Based on this data and the extensive knowledge on human glycosylation, this fucose residue has been assigned as an α1,6-linked core fucose. In addition, no diagnostic fragment ions indicative of nonreducing end fucosylation (*i.e.* sialyl $Lewis^{x/a}$ (*m/z* 801/819) and $Lewis^{x/a}$ (*m/z* 510/528)), were observed in LC-MS/MS experiments of CBG *N*-glycans without and with neuraminidase treatment; however, the presence of trace amount of Lewis-type fucosylation cannot be completely ruled out.

Several lines of indications supported the assignment of high branching structures of the CBG *N*-glycans (tri-, tetra-, and penta-/tetra antennary + one LacNAc extension) as opposed to repeating LacNAc units on structures showing a low degree of branching: 1) the agreement of the proposed number of antennas and the number of observed NeuAc-α2,3-Gal residues on the abundant structures (*i.e.* BS2 and TS3), 2) observation of structures with three, four, and five terminal GlcNAc residues from experiments where sequential digestion with neuraminidase and β-1,4-specific galactosidase was performed (supplemental Fig. S3), 3) observation of CBG *N*-glycans with three or more antennas by methylation analysis/gas chromatography analysis (14), and 4) the lack of retention on concanavalin A columns as reported by others (13). Interestingly, a minor proportion of the Gal residues could not be released by the β-1,4-specific galactosidase treatment. Fragment ions formed by cross-ring cleavages strongly indicated that this subset (10–15%, calculation not shown) contained β-1,3-linked Gal and that these were located in the nonreducing end (supplemental Fig. S3). Together, this confirms that CBG *N*-glycans are predominantly of the highly branched form. However, a trace amount of structures with repeated LacNAc extensions in particular for *N*-glycans with five LacNAc units cannot be excluded.

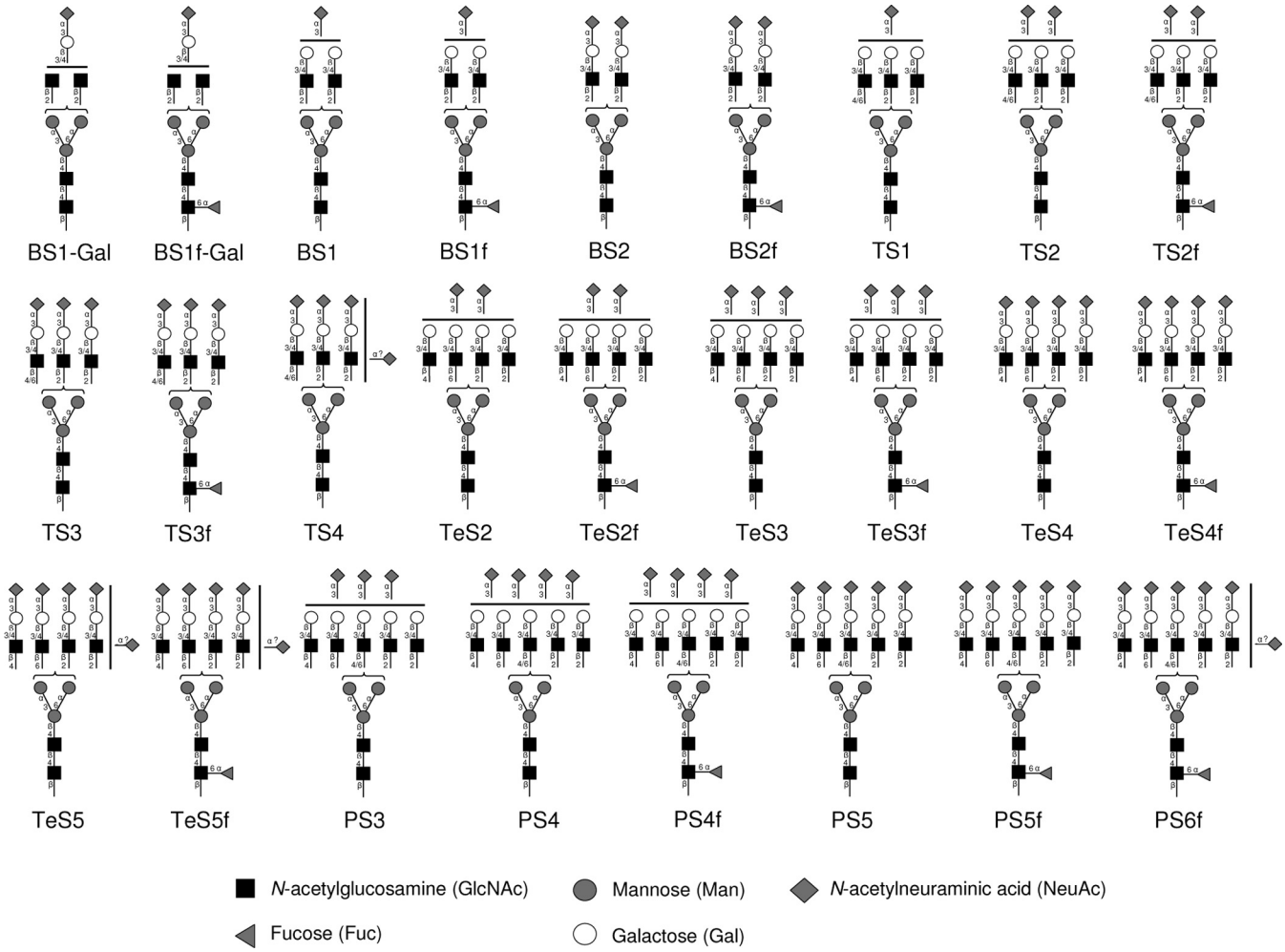

FIG. 3. **The complete set of observed CBG *N*-glycans.** B, bi-antennary; T, tri-antennary; Te, tetra- antennary; P, penta-/tetra- + one LacNAc antennary; S, NeuAc; f, fucose; Gal, galactose. Likely linkages and topologies are specified based on experimental data and general knowledge of human *N*-glycosylation. Brackets means that the antennae position on the α1,3- or α1,6-mannose arm is unknown. Similarly, the locations of NeuAc residues have not been specified on the antennas in case of under-sialylation and over-sialylation. Due to their low abundance it cannot be excluded that *N*-glycans with five LacNAc units attached to the core appeared as an isomeric mixture of penta-antennary and tetra-antennary structures with one LacNAc extension. Here, these structures are shown as penta-antennary *N*-glycans due to evidence from fragmentation and glycosidase experiments (supplemental Fig. S3).

Based on the obtained information and the general knowledge of human *N*-glycosylation, the observed 26 CBG *N*-glycans are illustrated in Fig. 3 with linkage positions and type. Brackets have been made to indicate that the position of the antennae on the two mannose arms is unknown. Similarly, the location of NeuAc residues has not been specified on the antennas in case of under- and over-sialylation.

CBG Glycosylation Analogs—To investigate the role of the CBG *N*-glycans, a set of glycosylation analogs was generated and tested with a functional assay. The glycosylation analogs were produced by glycosidase treatment of CBG under native conditions (20 mM Tris-HCl, pH 7.4) to generate a set of CBG isoforms that varied only in glycosylation, while retaining its mature protein conformation. Specifically, four CBG analogs were produced: Partially deglycosylated CBG (CBG_{Degly}), two partially desialylated CBG variants ($CBG_{Desia\ 1}$ and $CBG_{Desia\ 2}$) and a completely deglycosylated CBG molecule ($CBG_{Desia/Degly}$). As a control, CBG was incubated under the same conditions as the glycosylation analogs, but without enzyme (CBG_{Incub}), to prove that it was structurally identical to native CBG (CBG_{Nat}) following heat exposure. Importantly, the glycosylation analogs were all incubated for the same total amount of time (*i.e.* 39 h at 37 °C), but with different incubation times in the presence of the enzymes. None of the CBG analogs showed visual signs of precipitation, but a minor degree of precipitation and desolubilization cannot be excluded. The analogs were monitored using SDS-PAGE and MALDI MS intact mass, Fig. 4. Both CBG_{Nat} and CBG_{Incub} showed molecular masses of ~52–56 kDa as previously reported (5). The multiple gel bands and broadness of the intact mass peaks indicated heterogeneity of the glycosylation analogs. It appeared that two to three *N*-glycans were removed

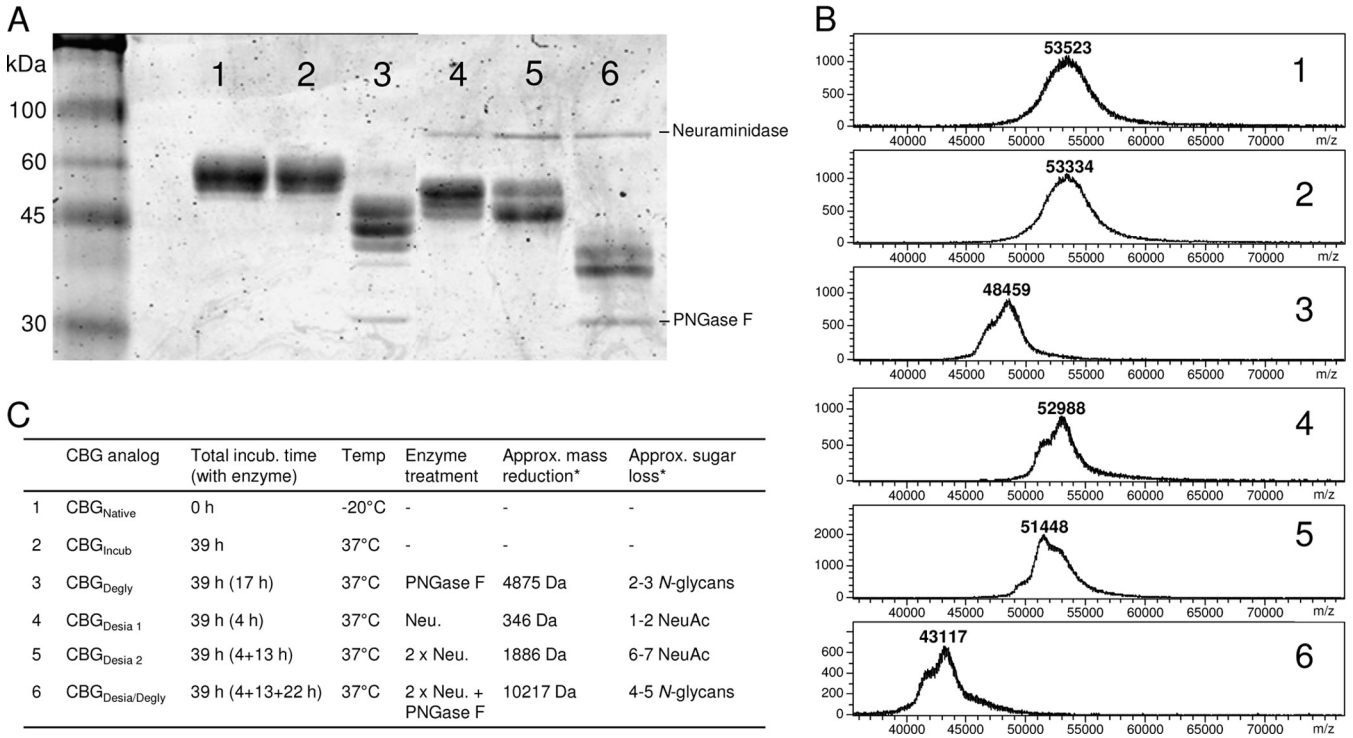

C

	CBG analog	Total incub. time (with enzyme)	Temp	Enzyme treatment	Approx. mass reduction*	Approx. sugar loss*
1	CBG_{Native}	0 h	-20°C	-	-	-
2	CBG_{Incub}	39 h	37°C	-	-	-
3	CBG_{Degly}	39 h (17 h)	37°C	PNGase F	4875 Da	2-3 *N*-glycans
4	$CBG_{Desia\ 1}$	39 h (4 h)	37°C	Neu.	346 Da	1-2 NeuAc
5	$CBG_{Desia\ 2}$	39 h (4+13 h)	37°C	2 x Neu.	1886 Da	6-7 NeuAc
6	$CBG_{Desia/Degly}$	39 h (4+13+22 h)	37°C	2 x Neu. + PNGase F	10217 Da	4-5 *N*-glycans

FIG. 4. **Generation of glycosylation analogs.** A number of CBG glycosylation analogs were produced by treatment with glycosidases. These analogs were monitored using SDS-PAGE (*A*) and intact mass MALDI MS (*B*). 1–6 refer to the following CBG variants: 1) Native CBG (CBG_{Native}), 2) Heat exposed CBG (CBG_{Incub}), 3) Partially deglycosylated CBG (CBG_{Degly}), 4, 5) Partially desialylated CBG (CBG_{Desia1} and CBG_{Desia2}), 6: Completely deglycosylated CBG ($CBG_{Desia/Degly}$). Specific conditions for the generations of the glycosylation analogs are provided in (*C*) and *Experimental Procedure*. *The approximate mass reduction and the corresponding sugar loss as compared with CBG_{Incub}.

from $CBG_{Degly\ 1}$, two to three and six to seven NeuAc residues were removed from $CBG_{Desia\ 1}$ and $CBG_{Desia\ 2}$, respectively and that $CBG_{Desia/Degly}$ was largely stripped of *N*-glycans.

Validation of the Functional Assay—The functional assay was based on the observation that MCF-7 cells produce cAMP as a second messenger when CBG interacts with its cell surface receptor (12). Thus, the cAMP amount can be used to monitor the CBG:receptor interaction and the assay for this has been thoroughly validated (12). Initially, we confirmed that cAMP is produced in a dose- (CBG) and time-dependent manner when MCF-7 cells were challenged with CBG (data not shown). It was also established that addition of cortisol to CBG was required in the assay because no significant cAMP was produced upon challenge with CBG or cortisol alone (12). First, MCF-7 cells (4.5×10^5 cells/challenge) were challenged with equal amounts of CBG_{Nat} and CBG_{Incub} to investigate whether heat exposure (*i.e.* 39 h at 37 °C) changed the ability of CBG to bind to its receptor and produce cAMP. Using EIA measurements, the cAMP amounts were determined to be 71.4 ± 18.9 fmol/4.5×10^5 cells with CBG_{Nat} (mean ± S.E. are shown for all cAMP measurements, $n = 6$ except otherwise stated) and 38.5 ± 4.5 fmol/4.5×10^5 cells with CBG_{Incub} ($n = 15$), showing that CBG clearly loses some receptor binding properties as a consequence of heat exposure. However, CBG_{Incub} retained measurable binding activity as shown by a cAMP response significantly higher ($p < 0.05$) than the constitutive level at 27.7 ± 3.5 fmol/4.5×10^5 cells ($n = 4$), Fig. 5.

Functional Characterization of CBG N-Glycans—Following validation of the functional assay, the receptor binding abilities of the glycosylation analogs were determined. Interestingly, CBG_{Degly} induced a cAMP response that was significantly higher than CBG_{Incub} *i.e.* 56.2 ± 5.5 fmol/4.5×10^5 cells, illustrating that the removal of two to three CBG *N*-glycans enhanced the CBG:receptor interaction. Challenge with $CBG_{Desia\ 1}$ produced a cAMP level that was higher, but not significantly higher, than CBG_{Incub} *i.e.* 49.8 ± 6.8 fmol/4.5×10^5 cells, whereas $CBG_{Desia\ 2}$ gave rise to a significantly higher cAMP response *i.e.* 57.1 ± 4.1 fmol/4.5×10^5 cells. Thus, removing few (two to three) NeuAc residues of CBG provided no significant enhancement of receptor binding, whereas releasing six to seven NeuAc residues provided enhanced CBG:receptor interaction. As expected from this set of observations, challenge with the fully deglycosylated $CBG_{Desia/Degly}$ produced an even higher cAMP level *i.e.* 63.0 ± 8.7 fmol/4.5×10^5 cells further proving the involvement of CBG *N*-glycans in the receptor binding. Importantly, it was confirmed that the individual glycosidases did not generate cAMP responses above the background level after incubation under similar conditions (data not shown). In ad-

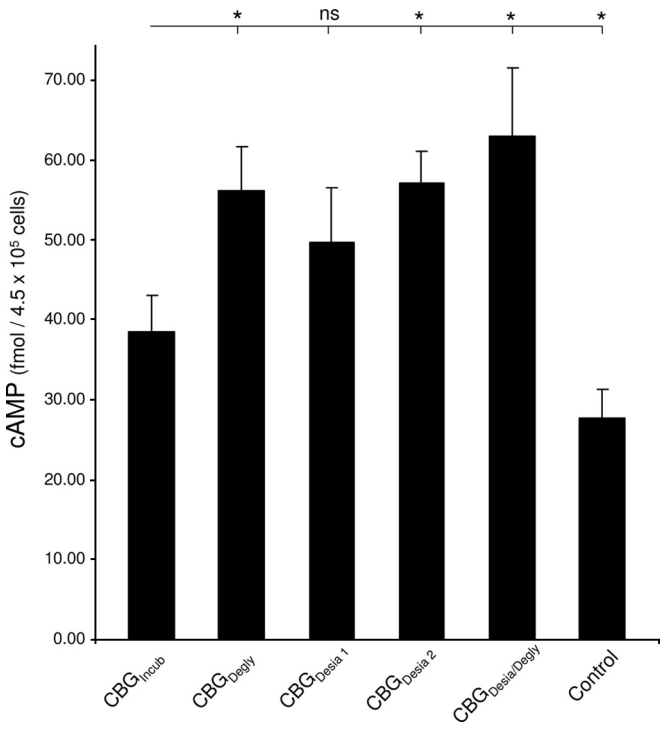

FIG. 5. **Involvement of *N*-glycans in the CBG:receptor interaction.** Bar graph showing the cAMP level of MCF-7 cells upon challenge with CBG and related glycosylation analogs. Mean and S.E. are shown and $n = 6$ for all analogs except for CBG_{Incub}, where $n = 15$ and the negative control sample containing 20 mM Tris-HCl, pH 7.4 ("Control"), where $n = 4$. The cAMP level for CBG_{Incub} was compared with the cAMP values for the other glycosylation analogs using a Student's *t* test with one tail, type 3. '*' indicates $p < 0.05$. ns: not significant.

dition, it is worth noting that any destabilization or desolubilization of CBG upon desialylation and deglycosylation as reported for other glycoproteins (47, 48) would lower the cAMP response. Taking this into consideration, the increased cAMP responses upon challenge with the glycosylation analogs may be actually somewhat under-estimated.

Altogether, this demonstrated that *N*-glycans are modulating the CBG:receptor interaction and that the CBG *N*-glycans and more specifically the NeuAc residues are restricting the interaction between the molecules.

DISCUSSION

CBG is a highly glycosylated protein and the energy expense associated with the addition (and regulation) of oligosaccharide post-translational modifications is significant. Thus, it seems reasonable to hypothesize that the *N*-glycans are important for the structure and function relationship of CBG. We have addressed this by performing a detailed structural characterization of the CBG *N*-glycans, and through functional assays investigated the importance of the *N*-glycans for CBG function. The nature of this study compelled us to use CBG purified from pooled human serum, giving an "average" CBG glycoprofile. However, it is likely that individual- and condition-specific CBG glycosylation occur and that the specific function of CBG glycosylation may be dependent of this variation for regulation purposes. We are currently investigating this aspect.

The structural characterization of the CBG *N*-glycans was predominantly performed using glycoproteomic techniques to obtain glycosylation site-specific information. This proved essential as the six *N*-glycosylation sites were very differently glycosylated. Although the glycoforms from the individual sites were similar and clearly followed the same synthetic pathway (*i.e.* all were sialylated complex type *N*-glycans), the degree of glycan processing was evidently site-specific. The similarities arise because the *N*-glycans on the individual sites are synthesized in the same secretory pathway and are thus processed similarly. Interestingly, the site-specific differences in the extent of glycan processing could be correlated with the position of the glycosylation sites on the protein surface by allowing differential access of the glycosyltransferases to the individual glycosylation sites and glycan substrates, supplemental Fig. S4. This part of the glycan processing is thought to occur on the maturely folded glycoprotein in the Golgi apparatus (49) and any steric hindrance on the protein surface will naturally affect glycan processing relatively close to the protein surface (*e.g.* core-fucosylation) more than glycan processing far from the protein surface (*e.g.* sialylation). For example, glycoforms originating from the relatively accessible glycosylation site 2 (Asn^{74}, rel. accessibility: 1.00) and 3 (Asn^{154}, rel. accessibility: 0.80) of CBG contained a higher degree of fucosylation (*i.e.* 13.7% and 14.1%, respectively) and a higher degree of branching (*i.e.* B:T:Te:P, 21:35:41:3 and 76:21:2:0, respectively) than glycoforms from the more buried glycosylation site 4 (Asn^{238}, rel. accessibility: 0.28) and 5 (Asn^{308}, rel. accessibility: 0.23) (fucosylation: 0% and 4.7% and branching: 79:21:0:0 and 71:29:0:0, respectively). Unfortunately, the crystal structure of human CBG complexed with cortisol, on which this modeling is based, does not include glycosylation site 1 and 6. However, the high level of fucosylation (*i.e.* 34.9%) and branching (18:71:9:2) observed for glycoforms on glycosylation site 6 agree well with its position on a flexible and exposed loop. In contrast, the degree of sialylation did not seem to be affected by the differential accessibilities, see Table II. Instead the degree of sialylation appeared to be related with the degree of branching. Hence, the degree of glycan processing relative close to the protein surface can thus provide some spatial information on the local conformation of the protein surface around the glycosylation sites.

By modeling on the same structure, it was found that glycosylation site 4 is located close to the entrance to the steroid binding site, supplemental Fig. S5. The limited branching of the *N*-glycans on this site (*i.e.* bi- and tri-antennary structures) might be required to allow accessibility of the steroid to the binding site. In addition, no *N*-glycans from this site contained core-fucosylation, which also may block the entrance to the

steroid binding site if present. Thus, the *N*-glycans attached to this site are potentially involved in the regulation of the accessibility of the steroid to its binding site, in addition to being required for the formation of the steroid binding site during folding of CBG (25–27).

The function of the CBG *N*-glycans was investigated with an assay that indirectly determines the binding of CBG to its cell surface receptor by measuring the amount of cAMP produced by MCF-7 cells upon challenge with native and glycan-modified CBG. The significant increase in cAMP production upon challenge with CBG_{Degly} as compared with CBG_{Incub} demonstrated that the *N*-glycans are modulating the CBG:receptor interaction and indicate that the *N*-glycans are limiting/shielding the CBG interaction with its receptor. A similar increase of the CBG:receptor interaction could be obtained by removing approximately six to seven NeuAc residues ($CBG_{Desia\ 2}$). This pinpoints the NeuAc residues of the CBG *N*-glycans as being responsible for restricting the CBG:receptor interaction and indicates that this interference may be caused not only by steric hindrance, but possibly also by electrostatic means. This agrees well with the observation that the CBG receptor also has been reported to be sialylated (8), thus enabling electrostatic repulsions between the molecules. The fine-tuning mechanism of the *N*-glycan in regulating the CBG:receptor interaction could in this case be controlled both by the degree of sialylation and by the extensive branching. This, in turn, is regulated by the abundance, localization, and activity of the involved glycosyltransferases, the ER/Golgi trafficking time and the availability of nucleotide-sugars. Understanding how the *N*-glycans influence the CBG:receptor interaction at a higher resolution is difficult because the binding site of human CBG to its receptor remains to be determined. However, considering the relative small size of CBG (42 kDa, protein mass only) it is likely that the binding site will be in proximity to at least one of the six *N*-glycans covering a large proportion of the CBG surface. In addition, the three-dimensional structure available for human CBG was produced from a crystal of nonglycosylated modified CBG (*i.e.* truncated protein with replacement of the reactive loop) making structural modeling potentially inaccurate. We are currently trying to map the receptor binding site of CBG and to specify the localization of the released *N*-glycans/NeuAc residues of the glycosylation analogs used in this study. For the latter, it is anticipated that the most accessible *N*-glycans/NeuAc residues were preferentially released because the deglycosylation/desialylation was performed under native conditions.

Post CBG receptor binding events include (1) CBG/cortisol complex internalization (12, 50, 51) (2) cortisol delivery to target cells (2, 52) and (3) cAMP second messenger generation (12). Such a variety of functions most likely result from the involvement of different receptors and CBG *N*-glycosylation could play a pivotal role in regulating which set of receptors are interacting with CBG. This working hypothesis is very plausible because the physicochemical properties of a number of CBG receptors are distinct (9, 10, 22, 53) suggesting they are different, and as previously discussed, the CBG *N*-glycans change under different hormonal states of an individual (16–21). Steroid hormone action could be targeted specifically to cells displaying a particular CBG receptor able to bind CBG that is showing a particular *N*-glycan profile.

In addition to the receptor binding property, the other major function of CBG is to bind, transport and release corticosteroids at appropriate locations in the organism. The binding of steroid is done in a defined binding pocket of CBG and the release is known to be induced by a conformational change of CBG promoted by a loop cleavage by elastase (5, 6). CBG *N*-glycans are potentially involved in both of these processes by regulating the accessibility of steroid to the binding pocket and defining its local conformation (see previous discussion) as well as possibly regulating the accessibility of elastase to the reactive center loop. For the latter, the elastase cleavage site between Val^{344}-Thr^{345} is interestingly located in close proximity to glycosylation site 6 at Asn^{347}. Hence, *N*-glycans from this site are likely affecting the accessibility of elastase to the cleavage site and may therefore be involved in the regulation of steroid release from CBG. Other functional assays will be needed to investigate if the CBG *N*-glycans, in addition to affecting the CBG:receptor interaction as demonstrated here, are also involved in the corticosteroid binding/release.

This study has shown that CBG is site-specifically glycosylated, apparently through differential accessibilities of glycosylation enzymes to the glycosylation sites. The *N*-glycans on CBG were shown to modulate its function, specifically by restricting the binding of CBG to its receptor.

Acknowledgment—We thank Lasse Dissing-Olesen for stimulating manuscript feedback and fruitful discussions.

* Morten Thaysen-Andersen was supported by The Danish Council for Independent Research Natural Sciences.

S This article contains supplemental Figs. S1 to S5.

‖ To whom correspondence should be addressed: Department of Chemistry and Biomolecular Sciences, Building E8C, Room 306, Macquarie University, NSW 2109, Australia. Tel.: +61 2 9850 7487; Fax: +61 2 9850 6192; E-mail: morten.andersen@mq.edu.au.

¶ Present address: Max Planck Institute of Colloids and Interfaces, Department of Biomolecular Systems Arnimallee 22, 14195 Berlin, Germany.

REFERENCES

1. Dunn, J. F., Nisula, B. C., and Rodbard, D. (1981) Transport of steroid hormones: binding of 21 endogenous steroids to both testosterone-binding globulin and corticosteroid-binding globulin in human plasma. *J. Clin. Endocrinol. Metab.* **53,** 58–68
2. Rosner, W. (1990) The functions of corticosteroid-binding globulin and sex hormone-binding globulin: recent advances. *Endocr. Rev.* **11,** 80–91
3. Hammond, G. L., Smith, C. L., Goping, I. S., Underhill, D. A., Harley, M. J., Reventos, J., Musto, N. A., Gunsalus, G. L., and Bardin, C. W. (1987) Primary structure of human corticosteroid binding globulin, deduced from hepatic and pulmonary cDNAs, exhibits homology with serine protease inhibitors. *Proc. Natl. Acad. Sci. U.S.A.* **84,** 5153–5157
4. Zhou, A., Wei, Z., Stanley, P. L., Read, R. J., Stein, P. E., and Carell, R. W. (2008) The S-to-R transition of corticosteroid-binding globulin and the mechanism of hormone release. *J. Mol. Biol.* **380,** 244–251

5. Hammond, G. L., Smith, C. L., Paterson, N. A., and Sibbald, W. J. (1990) A role for corticosteroid-binding globulin in delivery of cortisol to activated neutrophils. *J. Clin. Endocrinol. Metab.* **71,** 34–39
6. Klieber, M. A., Underhill C., Hammond, G. L., and Muller, Y. A. (2007) Corticosteroid-binding globulin, a structural basis for steroid transport and proteinase-triggered release. *J. Biol. Chem.* **282,** 29594–29603
7. Strel'chyonok, O. A., and Avvakumov, G. V. (1983) Evidence for the presence of specific binding sites for transcortin in human liver plasma membranes. *Biochim. Biophys. Acta* **755,** 514–517
8. Strel'chyonok, O. A., and Avvakumov, G. V. (1991) Interaction of human CBG with cell membranes. *J. Steroid. Biochem. Mol. Biol.* **40,** 795–803
9. Hryb, D. J., Khan, M. S., Romas, N. A., and Rosner, W. (1986) Specific binding of human corticosteroid-binding globulin to cell membranes. *Proc. Natl. Acad. Sci. U.S.A.* **83,** 3253–3256
10. Avvakumov, G. V., Krupenko, S. A., and Strel'chyonok, O. A. (1989) Study of the transcortin binding to human endometrium plasma membrane. *Biochim. Biophys. Acta* **984,** 143–150
11. Rosner, W., Hryb, D. J., Khan, M. S., Singer, C. J., and Nakhla, A. M. (1988) Are corticosteroid-binding globulin and sex hormone-binding globulin hormones? *Ann. N.Y. Acad. Sci.* **538,** 137–145
12. Nakhla, A. M., Khan, M. S., and Rosner, W. (1988) Induction of adenylate cyclase in a mammary carcinoma cell line by human corticosteroid-binding globulin. *Biochem. Biophys. Res. Com.* **153,** 1012–1018
13. Strel'chyonok, O. A., Avvakumov, G. V., Matveentseva, I. V., Akhrem, L. V., and Akhrem, A. A. (1982) Isolation and characterization of glycopeptides of human transcortin. *Biochim. Biophys. Acta* **705,** 167–173
14. Akhrem, A. A., Avvakumov, G. V., Akhrem, L. V., Sidorova, I. V., and Strel'chyonok, O. A. (1982) Structural organization of the carbohydrate moiety of human transcortin as determined by methylation analysis of the whole glycoprotein. *Biochim. Biophys. Acta* **714,** 177–180
15. Hammond, G. L., Smith, C. L., and Underhill, D. A. (1991) Molecular studies of corticosteroid binding globulin structure, biosynthesis and function. *J. Steroid. Biochem. Molec. Biol.* **40,** 755–762
16. Mihrshahi, R., Lewis, J. G., and Ali, S. O. (2006) Hormonal effects on the secretion and glycoform profile of corticosteroid-binding globulin. *J. Steroid. Biochem. Mol. Biol.* **101,** 275–285
17. Berdusco, E. T., Hammond, G. L., Jacobs, R. A., Grolla, A., Akagi, K., Langlois, D., and Challis, J. R. (1993) Glucocorticoid-induced increase in plasma corticosteroid-binding globulin levels in fetal sheep is associated with increased biosynthesis and alterations in glycosylation. *Endocrinology* **132,** 2001–2008
18. Avvakumov, G. V., and Strel'chyonok, O. A. (1987) Properties and serum levels of pregnancy-associated variant of human transcortin. *Biochim. Biophys. Acta* **925,** 11–16
19. Mitchell, E., Torpy, D. J., and Bagley, C. J. (2004) Pregnancy-associated corticosteroid-binding globulin: high resolution separation of glycan isoforms. *Horm. Metab. Res.* **36,** 357–359
20. Strel'chyonok, O. A., Avvakumov, G. V., and Akhrem, A. A. (1984) Pregnancy-associated molecular variants of human serum transcortin and thyroxine-binding globulin. *Carbohydrate Res.* **134,** 133–140
21. Blithe, D. L., Khan, M. S., and Rosner, W. (1992) Comparison of the carbohydrate composition of rat and human corticosteroid-binding globulin: species specific glycosylation. *J. Steroid Biochem. Mol. Biol.* **42,** 475–478
22. Avvakumov, G. V., and Strel'chyonok, O. A. (1988) Evidence for the involvement of the transcortin carbohydrate moiety in the glycoprotein interaction with the plasma membrane of human placental syncytiotrophoblast. *Biochim. Biophys. Acta* **938,** 1–6
23. Strel'chyonok, O. A., and Avvakumov, G. V. (1990) Specific steroid-binding glycoproteins of human blood plasma: novel data on their structure and function. *J. Steroid Biochem.* **35,** 519–534
24. Ghose-Dastidar, J., Ross, J. B., and Green, R. (1991) Expression of biologically active human corticosteroid binding globulin by insect cells: acquisition of function requires glycosylation and transport. *Proc. Natl. Acad. Sci. U.S.A.* **88,** 6408–6412
25. Avvakumov, G. V., and Hammond, G. L. (1994) Glycosylation of human corticosteroid-binding globulin. Differential processing and significance of carbohydrate chains at individual sites. *Biochemistry* **33,** 5759–5765
26. Avvakumov, G. V., Warmels-Rodenhiser, S., and Hammond, G. L. (1993) Glycosylation of human corticosteroid-binding globulin at aspargine 238 is necessary for steroid binding. *J. Biol. Chem.* **268,** 862–866
27. Avvakumov, G. V. (1995) Structure and function of corticosteroid-binding globulin: role of carbohydrates. *J. Steroid Biochem. Molec. Biol.* **53,** 515–522
28. Hossner, K. L., and Billiar, R. B. (1981) Plasma clearance and organ distribution of native and desialylated rat and human transcortin: species specificity. *Endocrinology* **108,** 1780–1786
29. Murata, Y., Sueda, K., Seo, H., and Matsui, N. (1989) Studies on the role of glycosylation for human corticosteroid-binding globulin: comparison with that for thyroxine-binding globulin. *Endocrinology* **125,** 1424–1429
30. Rudd, P. M., and Dwek, R. A. (1997) Glycosylation: heterogeneity and the 3D structure of proteins. *Crit. Rev. Biochem. Mol. Biol.* **32,** 1–100
31. Parekh, R. B., Tse, A. G., Dwek, R. A., Williams, A. F., and Rademacher, T. W. (1987) Tissue-specific N-glycosylation, site-specific oligosaccharide patterns and lentil lectin recognition of rat Thy-1. *EMBO J.* **6,** 1233–1244
32. Sheares, B. T., and Robbins, P. W. (1986) Glycosylation of ovalbumin in a heterologous cell: analysis of oligosaccharide chains of the cloned glycoprotein in mouse L cells. *Proc. Natl. Acad. Sci. U.S.A.* **83,** 1993–1997
33. Thaysen-Andersen, M., Thøgersen, I. B., Nielsen, H. J., Lademann, U., Brünner, N., Enghild, J. J., and Højrup, P. (2007) Rapid and individual-specific glycoprofiling of the low abundance N-glycosylated protein tissue inhibitor of metalloproteinases-1. *Mol. Cell. Proteomics* **6,** 638–647
34. Mysling, S., Palmisano, G., Højrup, P., and Thaysen-Andersen, M. (2010) Utilizing ion-pairing hydrophilic interaction chromatography solid phase extraction for efficient glycopeptide enrichment in glycoproteomics. *Anal. Chem.* **82,** 5598–5609
35. Wilson, N. L., Robinson, L. J., Donnet, A., Bovetto, L., Packer, N. H., and Karlsson, N. G. (2008) Glycoproteomics of milk: differences in sugar epitopes on human and bovine milk fat globule membranes. *J. Proteome Res.* **7,** 3687–3696
36. Gobom, J., Nordhoff, E., Mirgorodskaya, E., Ekman, R., and Roepstorff, P. (1999) Sample purification and preparation technique based on nano-scale reversed-phase columns for the sensitive analysis of complex peptide mixtures by matrix-assisted laser desorption/ionization mass spectrometry. *J. Mass. Spectrom.* **34,** 105–116
37. Papac, D. I., Wong, A., and Jones, A. J. (1996) Analysis of acidic oligosaccharides and glycopeptides by matrix-assisted laser desorption/ionization time-of-flight mass spectrometry. *Anal. Chem.* **68,** 3215–3223
38. Thaysen-Andersen, M., Mysling, S., and Højrup, P. (2009) Site-specific glycoprofiling of N-linked glycopeptides using MALDI-TOF MS: strong correlation between signal strength and glycoform quantities. *Anal. Chem.* **81,** 3933–3943
39. Stadlmann, J., Pabst, M., Kolarich, D., Kunert, R., and Altmann, F. (2008) Analysis of immunoglobulin glycosylation by LC-ESI-MS of glycopeptides and oligosaccharides. *Proteomics* **8,** 2858–2871
40. Hubbard, S. J., and Thornton, J. M. (1993) NACCESS computer program, http://wolf.bms.umist.ac.uk/naccess/, Department of Biochemistry and Molecular Biology, University College London
41. Lee, B., and Richards, F. M. (1971) The interpretation of protein structures: estimation of static accessibility. *J. Mol. Biol.* **55,** 379–400
42. Chothia, C. (1976) The nature of the accessible and buried surfaces in proteins. *J. Mol. Biol.* **105,** 1–12
43. Hogan, J. M., Pitteri, S. J., Chrisman, P. A., and McLuckey, S. A. (2005) Complementary structural information from a tryptic N-linked glycopeptide via electron transfer ion/ion reactions and collision-induced dissociation. *J. Proteome Res.* **4,** 628–632
44. Deshpande, N., Jensen, P. H., Packer, N. H., and Kolarich, D. (2010) GlycoSpectrumScan: fishing glycopeptides from MS spectra of protease digests of human colostrum sIgA. *J. Proteome Res.* **9,** 1063–1075
45. Pabst, M., Bondili, J. S., Stadlmann, J., Mach, L., and Altmann, F. (2007) Mass + retention time = structure: a strategy for the analysis of N-glycans by carbon LC-ESI-MS and its application to fibrin N-glycans. *Anal. Chem.* **79,** 5051–5057
46. Green, E. D., Adelt, G., Baenziger, J. U., Wilson, S., and Van Halbeek, H. (1988) The asparagine-linked oligosaccharides on bovine fetuin. Structural analysis of N-glycanase-released oligosaccharides by 500-megahertz 1H NMR spectroscopy. *J. Biol. Chem.* **263,** 18253–18268
47. Dissing-Olesen, L., Thaysen-Andersen, M., Meldgaard, M., Højrup, P., and Finsen, B. (2008) The function of the human interferon-beta 1a glycan

determined in vivo. *J. Pharm. Exp. Therap.* **326,** 338–347
48. Grimaldi, S., Robbins, J., and Edelhoch, H. (1985) Interaction of carbohydrate and protein in thyroxine binding globulin. *Biochemistry* **24,** 3771–3776
49. Trombetta, E. S. The contribution of N-glycans and their processing in the endoplasmic reticulum to glycoprotein biosynthesis. *Glycobiology* 13(9): 77R-91R, 2003
50. Hsu, B. R.-S., Siiteri, P. K., and Kuhn, R. W. (1986) In: *Binding proteins of steroid hormones,* (Forest, M.G., and Pugeat, M. Eds) pp 577–591, John Libbey, London
51. Kuhn, R. W. (1988) Corticosteroid-binding globulin interactions with target cells and plasma membranes. *Ann. N.Y. Acad. Sci.* **538,** 146–158
52. Singer, C. J., Khan, M. S., and Rosner, W. (1988) Characteristics of the binding of corticosteroid-binding globulin to rat cell membranes. *Endocrinology* **122,** 89–96
53. Avvakumov, G. V., Krupenko, S. A., Dubovskaia, L. V., and Strel'chenok, O. A. (1988) Interaction of the transcortin-progesterone complex with plasma membranes of human decidual epithelium. *Biokhimiia* **53,** 586–590

In order to cite this article properly, please include all of the following information: Sumer-Bayraktar, Z., Kolarich, D., Campbell, M. P., Ali, S., Packer, N. H., and Thaysen-Andersen, M. (2011) *N*-Glycans Modulate the Function of Human Corticosteroid-Binding Globulin. *Mol. Cell. Proteomics* 10(8):M111.009100. DOI: 10.1074/mcp.M111.009100.